BRAIN
ORIGINAL ARTICLE

APOE4 derived from astrocytes leads to blood–brain barrier impairment

Rosemary J. Jackson,[1,2] Jonah C. Meltzer,[1,2,†] Huong Nguyen,[1,2,†] Caitlin Commins,[1,2] Rachel E. Bennett,[1,2] Eloise Hudry[1,2,3] and Bradley T. Hyman[1,2]

†These authors contributed equally to this work.

Apolipoprotein E (ApoE) is a multifaceted secreted molecule synthesized in the CNS by astrocytes and microglia, and in the periphery largely by the liver. ApoE has been shown to impact the integrity of the blood–brain barrier, and, in humans, the *APOE4* allele of the gene is reported to lead to a leaky blood–brain barrier. We used allele specific knock-in mice expressing each of the common (human) ApoE alleles, and longitudinal multiphoton intravital microscopy, to directly monitor the impact of various ApoE isoforms on blood–brain barrier integrity.

We found that humanized *APOE4*, but not *APOE2* or *APOE3*, mice show a leaky blood–brain barrier, increased MMP9, impaired tight junctions, and reduced astrocyte end-foot coverage of blood vessels. Removal of astrocyte-produced ApoE4 led to the amelioration of all phenotypes while the removal of astrocyte-produced ApoE3 had no effect on blood–brain barrier integrity.

This work shows a cell specific gain of function effect of ApoE4 in the dysfunction of the BBB and implicates astrocyte production of ApoE4, possibly as a function of astrocytic end foot interactions with vessels, as a key regulator of the integrity of the blood–brain barrier.

1 Alzheimer Research Unit, The Massachusetts General Hospital Institute for Neurodegenerative Disease, Charlestown, MA, USA
2 Department of Neurology, The Massachusetts General Hospital and NeuroDiscovery Center, Harvard Medical School, Boston, MA, USA
3 Novartis Institute for Biomedical Research, Cambridge, MA, USA

Correspondence to: Bradley Hyman
Massachusetts General Hospital MIND Institute
114 16th Street, Charlestown, 02129 MA, USA
E-mail: bhyman@mgh.harvard.edu

Introduction

The blood–brain barrier (BBB) is a highly selective semipermeable barrier that allows for specific influx and efflux of nutrients and wastes in the brain. The vascular unit within the CNS is comprised predominantly of endothelial cells, pericytes, and astrocytes. Dysfunction of this tightly organized unit is impacted by ageing as well as a number of neurodegenerative diseases.[1–4]

Apolipoprotein E (ApoE) is the most abundant apolipoprotein in the CNS. It is produced both in the periphery and in the brain and early studies showed that these two pools of ApoE rarely mix.[5] Within the CNS, ApoE is predominantly produced by astrocytes

with contributions also made by other glial cells, especially microglia. In the periphery, ApoE is essentially produced within the liver.[6,7] There are three main isoforms of *APOE* carried by humans with the most common being *APOE3* followed by *APOE4* and then *APOE2*. *APOE4* is the greatest genetic risk factor for developing sporadic Alzheimer's disease but also is associated with an increased risk for atherosclerosis as well as other neurodegenerative diseases.[8] *APOE2* confers a protective effect against developing Alzheimer's disease but is associated with hyperlipoproteinaemia.[8]

ApoE is involved in brain vasculature regulation in both the presence and absence of overt, neurodegeneration related, pathology.[9] For example, ApoE4 is associated with reduced BBB repair following traumatic brain injury,[10] reduced tight junction proteins *in vitro*,[11] reduced pericyte coverage of blood vessels in human post-mortem tissue,[12] and increased leakage of the BBB in both mouse models and aged humans.[13,14] Studies in mouse models have shown that *Apoe* knockout animals also present with impairments in BBB function, indicating that it is essential for BBB formation or maintance.[15] Moreover, in the context of Alzheimer's disease, ApoE4 is associated with increased deposition of amyloid in vessel walls both in human congophilic amyloid angiopathy and in murine models,[16] potentially related to altered clearance mechanisms.

Astrocytes are an important part of the neurovascular unit providing support and signals to the BBB both in health and disease.[17] They are a major source of ApoE in the CNS. We therefore tested the hypothesis that astrocyte-derived ApoE4 would drive ApoE-dependent BBB alterations. To assess the effect of astrocyte-produced ApoE on BBB dysfunction, we used ALDH1L1-Cre/ERT2 BAC transgenic mice, in which the astrocyte-specific ALDH1L1 promoter drives expression of an inducible Cre recombinase, crossed with humanized floxed *APOE3* or *APOE4* mice, allowing for the conditional knockout of ApoE from astrocytes.[18,19] This allowed us to investigate whether removing astrocyte-produced ApoE would have an effect on BBB integrity, and whether the reduction of ApoE4 in astroglial cells could restore BBB homeostasis.

Materials and methods

Animals

Conditional humanized *APOE* knock-in (KI) mice[19] were used for the study. These mouse lines were generated by replacing the endogenous mouse gene from the initiation codon to the termination codon by its human counterparts (*APOE-E2*, *APOE-E3* and *APOE-E4*), flanking exons 2 to 4 with LoxP sites.[18,19] *Apoe* knockout (KO) mice were also used (The Jackson Laboratory). To generate mice with conditional knockout of huApoE in astrocytes, *APOE*-KI were crossed with tamoxifen inducible ALDH1L1-CRE mice (The Jackson Laboratory) for two successive generations to obtain heterozygous ALDH1L1-*Cre* mice homozygous for various *APOE* isoforms. Genotyping for *APOE* and ALDH1L1-CRE were performed by PCR following protocols given by The Jackson's Laboratory (*Apoe* KO, ALDH1L1-CRE) or Taconic (huAPOE). Mice are termed APOE2, APOE3, APOE4 and APOE KO throughout the paper. Mice that have undergone flox recombination are termed APOE3 astrocyte knockout (aKO) and APOE4 aKO. Mice were group-housed in accredited facilities with temperature and humidity controls and were under a 12-h light/dark cycle. Mice had access to food and water *ad libitum* throughout all phases of the experiments. All animal experiments were approved by the Massachusetts General Hospital Subcommittee on Research Animal Care following the guidelines set forth by the National Institutes of Health Guide for the Care and Use of Laboratory Animals.

Cranial window surgery

At 8–8.5 months old, mice were anaesthetized with isoflurane (1–1.5% in oxygen) and a cranial window was implanted by removing a piece of skull above the somatosensory cortex and replacing it with an 8 mm diameter cover glass (as described previously[20]). The cover glass was secured in place with dental cement mixed with crazy glue which allows for long term placement of the cover glass. After surgery, mice recovered for 3 weeks before imaging.

Two-photon imaging

Mice were anaesthetized with isoflurane (1–1.5%) in oxygen and the coverglass was cleaned with 70% ethanol. Mice were imaged on an Olympus FluoView FV1000MPE multiphoton laser scanning system mounted on an Olympus BX61WI microscope and an Olympus 25× dipping objective (NA = 1.05, Olympus), with the emission path shielded from external light contamination. A DeepSee Mai Tai Ti:sapphire mode-locked laser (Mai Tai; Spectra-Physics) generated two-photon excitation at 800 nm, and detectors containing three photomultiplier tubes (PMTs; Hamamatsu) collected emitted light in the range of 380–480, 500–540, and 560–650 nm. PMTs settings remained unchanged throughout the different imaging sessions, but laser power was adjusted as needed. Immediately prior to imaging 0.1 ml fluorescein conjugated 40 kDa dextran (1.5 mg/ml) was injected retro-orbitally. Two fields of view were captured every 10 min (Z-series, 508 μm × 508 μm, 2 μm slices, depth of 100–200 μm) per mouse for 30 min. Mice were kept warm on a heat pad during imaging and after imaging the mouse was allowed to recover on a heating pad and then returned to its home cage.

Two-photon image processing

All images were opened in grey scale and the intra and extravascular fluorescence intensity was measured using the NIH ImageJ Integrated Density measurement function by an investigator blind to genotype. The *in vivo* BBB permeability for dextran was calculated as the normalized leakage by $(I_t - I_0)/I_0 \times 100$ where I_0 is the fluorescence intensity within the parenchyma at time point 0 and I_t is the intensity at the measured time point for the same cerebral region of interest.

Tamoxifen injection

Mice were injected intraperitoneally at ~9.75 months of age with 100 mg/kg of tamoxifen (Tam) diluted to 20 mg/ml in corn oil or corn oil as a vehicle control. Mice were injected once per day for 4 days and were monitored. Mice were imaged for their second imaging session 1 week after the first day of tamoxifen injection. The third imaging session took place 1 month after tamoxifen injection and the fourth session occurred ~2 months after tamoxifen (for five mice the final imaging session was delayed or brought forward by 1 week due to COVID-19 shutdowns, mice were not imaged further than 1 week from their intended 2 month imaging date). Mice in which technical issues precluded further imaging were included in analysis for all imaging sessions accomplished and were culled and processed for biochemistry, electron microscopy and/or RNAscope.

Tissue collection

Mice were culled using lethal dose of isoflurane in oxygen. Blood was collected using an EDTA-coated needle via cardiac puncture and spun for 10 min at 1500*g* to obtain plasma. The mouse was

then perfused with ice-cold phosphate-buffered saline (PBS) and tissue collected for immunohistochemical and/or biochemical analysis. A 4 mm thick coronal slice was removed from the middle of the right hemisphere and fixed by immersion in 4% paraformaldehyde in PBS for 48 h before being embedded in paraffin while a 2 mm thick coronal slice was removed from the middle of the left hemisphere and fixed by immersion in 1% paraformaldehyde and 1% glutaraldehyde in 0.1 M sodium cacodylate before being processed for electron microscopy. The cerebellum was removed and snap frozen for DNA extraction while the remainder of the brain was snap frozen and processed for RNA and protein extraction. Due to the size of the mouse brain not all mice were processed for all analyses and *n* numbers fluctuated. Graphs display each individual mouse as a data-point and thus mouse numbers per genotype or condition are indicated by each experimental results graph.

PCR for monitoring Cre-dependent recombination

DNA was extracted from the cerebellum using the DNeasy blood and tissue kit (Qiagen) and its concentration measured on a NanoDrop spectrophotometer (ThermoFisher). A small fragment of DNA corresponding to the site of flox recombination was amplified using KAPA taq PCR master mix (Roche). The forward primer was GGGTTACCTCCAGGAAGGAG and the reverse primer was CTCGACCTTGTCCATGTCCT. The resulting product was run on a 2% agarose gel with ethidium bromide at 120 V in TAE buffer for 1 h and imaged using UV.

Blood vessel isolation

Blood vessels were isolated from frozen mouse tissue as described previously.[21,22] A ~200 mg piece of forebrain was minced into small pieces in ice cold buffer 1 Hanks Balanced Salt Solution (HBSS) with 10 mM HEPES, pH 7, and then manually homogenized using a dounce homogenizer. The homogenate was then transferred to a 50 ml conical tube containing 20 ml of Buffer 1 and centrifuged at 2000*g* for 10 min at 4°C. The supernatant was discarded and the pellet was resuspended by shaking in 20 ml of Buffer 2 (18% dextran in HEPES-buffered HBSS). Samples were centrifuged again at 4400*g* for 15 min at 4°C. Myelin was removed by carefully pouring out the supernatant and wiping the upper part of the tube with a kim wipe. The pellet was resuspended in 2 ml chilled 1% bovine serum albumin (BSA) HEPES-buffered HBSS and filtered through a 20 μm mesh (Millipore). The filter was rinsed with 30 ml 1% BSA HEPES-buffered HBSS and then blood vessels were collected by immersing the filter in a new conical containing 30 ml of the same buffer and shaking gently before centrifuging for 10 min at 2000*g* at 4°C. The pellet was resuspended in 1 ml of the same buffer, transferred to a 1.5 ml Eppendorf and centrifuged at 3000*g* for 10 min at 4°C. The buffer was removed and RNA was extracted from a section of forebrain using the RNeasy Mini Kit (Qiagen).

Quantitative PCR

RNA was extracted from a section of forebrain using the RNeasy Mini Kit (Qiagen) and was eluted in 80 μl of nuclease-free water. RNA was assessed using a NanoDrop spectrophotometer (ThermoFisher) and diluted to a standard concentration of 7.1 ng/μl for each sample. cDNA was synthesized using the QuantiTect Reverse Transcription kit (Qiagen) and was combined with RT^2 SYBR Green Mastermix fluorescent dye (Qiagen). Primers for *APOE* (QT00087297) *Gapdh* (QT00199388) *Gtfb*2 (QT00156569) and *Mmp9* (QT00108815) were ordered from Qiagen. Genes of interest (*APOE*

and *Mmp9*) were run alongside two housekeeping genes that were used to normalize for RNA amount. The plate was covered with a plastic seal to prevent sample evaporation and briefly spun at ~300*g* to remove bubbles. The qPCR reactions were performed using the BioRad CFX96 Real-Time Detection System. The sequence began with a 10-min incubation at 95°C to activate the DNA polymerase enzyme. Fluorescence data collection then commenced with 40 cycles of alternating 15 s at 95°C and 60 s at 60°C.

The ΔΔCT relative quantification method was used to calculate gene expression. Two reference genes were included in the RT^2-Profiler array: GTF2B and GAPDH. The geometric mean of the reference gene Ct values was calculated for each animal and subtracted from the Ct value of each target gene, yielding ΔCT values. For each gene, the average ΔCT value from APOE3 animals was then subtracted from each sample's ΔCT value to obtain ΔΔCT values. The relative quantification (RQ) value was calculated as $2^{-\Delta\Delta CT}$, which was then log2-transformed to yield fold changes.

RNAscope

Four mice per experimental condition were stained for *APOE* mRNA by RNAscope. RNAscope experiments were performed using the Manual Fluorescent Multiplex kit v2 (Advanced Cell Diagnostics) following manufacturer's recommendations with minor adjustments. Briefly for each mouse a single paraffin section was baked onto a superfrost slide for use in *APOE* mRNA quantification. Following deparaffinization, target retrieval and protease digestion, probe hybridization was carried out at 40°C for 2 h with hs-APOE (433091), 3-plex Positive Control Probe_Mm (320881) and Negative Control Probe- DapB (310043). After amplification steps to obtain the RNAscope signals, the signal was developed using TSA-cy3 (Perkin Elmer FP1170).

We then immediately performed immunohistochemistry. Sections were permeabilized in 0.5% Triton-X for 15 min before being blocked in 0.1% Triton-X and 5% normal goat serum for 1 h at room temperature. Primary antibodies GFAP (Millipore MAB 3402) was diluted 1:1000 in 0.05% and 2.5% normal goat serum overnight at 4°C. Secondary was goat anti-mouse 488 (Thermo-Fisher A11001) diluted 1:500 in 0.05% and 2.5% normal goat serum at room temperature for 1 h. Sections were then mounted using Vectashield Antifade mounting medium with DAPI (ZG0729) coverslipped and imaged on an Olympus FV3000 confocal laser scanning microscope.

Electron microscopy

Tissue slices were left in electron microscopy fix until ready to process. Tissue sections were then rinsed in PBS and secondarily fixed in 1% osmium tetroxide in 0.1 M sodium cacodylate overnight at room temperature. Sections were then rinsed in 0.1 M sodium cacodylate before being dehydrated through ascending concentrations of ethanol. Sections were then incubated with propylene oxide before being embedded and baked for 48 h in Poly/Bed® 812 at 60°C. Tissue was then sectioned on an Ultracut microtrome and post-stained with 2% uranyl acetate and lead citrate. Sections were then examined using a Philips 208S electron microscope (Philips), with images collected at ×5000, ×20 000 and ×50 000 magnification.

Western blots

Mouse cortical tissue was homogenized in 10 volumes by weight of ice-cold TBS with protease and phosphatase inhibitors using a hand-held electric homogenizer. The homogenate was then spun

at 10 000*g* for 10 min and the supernatant (TBS-soluble fraction) was collected for western blot. Protein concentration was determined using a BCA assay. Total protein (5–10 µg) was loaded and separated by 4–12% NuPAGE gels in MES buffer, proteins were then separated by weight for 2 h at 120 V. Proteins were electrotransferred onto nitrocellulose membrane at 30 V for 1.5 h using the XCell II™ Blot Module system in tris-glycine transfer buffer. Membranes were incubated in blocking buffer (Li-Cor Biosciences) diluted 1:1 TBS for 1 h to reduce background staining. Membranes were then incubated with primary antibodies; rb anti-ApoE (Novus biologicals, NBP1-31123), rb anti-MMP9 (abcam ab38898), ms anti-GAPDH (Millipore MAB374), ms anti-Tubulin (Abcam ab7291) diluted in blocking buffer with added 0.1% Tween-20 overnight at room temperature while shaking. Membranes were then washed and incubated with the appropriate 680 and 800 IR dye secondary antibodies (Li-Cor Biosciences). The membranes were imaged using Odyssey infrared imaging system, and analysed using Odyssey software.

Statistical analyses

Statistical analyses were performed using GraphPad Prism 9. Data are most often presented as mean ± standard error of the mean (SEM), where one dot is representative of one mouse. If multiple measurements were taken for an individual mouse at a single time point, as in the case of the leakage experiments or the electron microcsopy, all measurements per mouse were averaged together and then mice were compared using an ANOVA with *post hoc* Tukey's multiple comparisons test. The exception to this is Fig. 4C where all tight junction measured were compared to show the increased spread in APOE4 animals. Simple linear regression analysis was used to assess intensity over time and the correlation between gene expression.

Data availability

The data that support the findings of this study are available from the corresponding author, upon reasonable request.

Results

APOE4 animals show BBB disruption compared with APOE3 and APOE2 animals

To assess the effect of different *APOE* alleles on BBB integrity we used longitudinal *in vivo* multiphoton microscopy of humanized *APOE* floxed knock-in (APOE4, APOE3, APOE2, as a group referred to as APOE-KI) animals. Mice fitted with cranial windows were injected intravenously with 40 kDa fluorescein-labelled dextran, which does not passively cross the BBB to measurable levels in the APOE3 animals as shown by us and other groups.[13,23] Two z-stacks (508 µm × 508 µm × ∼120 µm) per mouse were taken within 3 min of injection of dextran dye as a baseline and then these same areas were imaged every 10 min for 30 min to assess leakage over time. Regions of interest were drawn and measured near capillaries (diameter < 10 µm) in the brain parenchyma in the same areas in each time point image and the intensity of each time point was compared with the baseline image as a per cent increase in fluorescence intensity. Six capillaries per area were also measured for intensity and width (Supplementary Fig. 1B and C) and, as expected, showed no differences between groups in capillary width and change in intraluminal intensity (Supplementary Fig. 1D).

We observed an increase in the extravasation of fluorescein-labelled 40 kDa dextran in the APOE4 mice but not APOE3 or APOE2 mice (Fig. 1A and B). We detected a progressive accumulation of dextran in the brain parenchyma over the 30 min imaged (Supplementary Fig. 1E). As matrix metallopeptidase 9 (MMP9) has been shown to be an important mediator of ApoE-dependent BBB deficits,[13] *Mmp9* transcription level in APOE-KI animals was determined by qPCR and we found that there is a significant increase (∼30%) in *Mmp9* transcript in APOE4 brains compared with APOE3 or APOE2 animals. (Fig. 1C), in accord with previous studies.[13] As expected, when we quantified the amount of MMP9 protein by western blot, there was an absolute increase in MMP9 protein in APOE4 compared with APOE2 and APOE3 animals (Fig. 1D).

Western blot analyses showed ∼15% less ApoE protein in the APOE4 animals as compared with the APOE2 and APOE3 mice. By contrast, there was no difference in the amount of *APOE* mRNA among the different APOE-KI animals, suggesting that ApoE4 protein may be degraded faster than other isoforms of the protein, in line with previous research suggesting faster turnover of ApoE4.[24]

Selective KO of ApoE4 from astrocytes rescues BBB integrity, yet Apoe KO mice show a BBB deficit

APOE4-KI mice have a defect in BBB integrity. We considered that this might be due to a gain of function or to a loss of function of ApoE4 compared to ApoE2 or ApoE3. To evaluate these possibilities, we first evaluated *Apoe* KO mice and found that they also showed a leaky BBB (Supplementary Fig. 2A and B). This would be consistent with a loss-of-function of ApoE4. We measured the amount of *Mmp9* mRNA and protein in the *Apoe* KO mice (Supplementary Fig. 2C and D) and found that while there is an increase in protein as compared with APOE3 animals there is no increase in mRNA levels indicating that this increase in MMP9 protein in *Apoe* KO and APOE4 mice could be due to two different mechanisms. Moreover, *Apoe* KO mice lack ApoE throughout development both in the CNS and in the periphery, and therefore the underlying molecular mechanisms compromising the integrity of the BBB in those animals may also differ from APOE4 mice. Thus, to further explore the question of whether ApoE4 leads to a gain- or loss-of-function effect on BBB integrity, we directly tested whether suppression of ApoE4 in astrocytes in the mature CNS increases, alleviates, or does not impact BBB leakage. We expected that, if ApoE4 had a loss-of-function effect, suppression of expression would not improve, and may even worsen, the BBB defect. By contrast, if suppression of ApoE4 in astrocytes rescues the BBB defect, a gain-of-function mechanism would be supported.

The mouse model used in the present study allows cell-type specific inducible knockout of ApoE. Tamoxifen induces expression of the recombinase CRE in ALDH1L1-positive astrocytes, causing the excision of *APOE*'s exons 2 to 4 and preventing the expression of ApoE in those cells.[18,19] This leads to the production of a DNA fragment that is only detected by PCR after flox sites recombination (Fig. 2A) and leads to a 40% reduction in CNS *APOE* mRNA levels by qPCR and a ∼50% reduction in ApoE protein levels by western blot 1 month and 2 months post-tamoxifen injection, although not at 1 week (Fig. 2B, D and E). RNAscope shows that GFAP positive astrocytes in the cortex of these mice no longer contain *APOE* mRNA (Fig. 2C). A slight reduction of ApoE protein was also detected in the plasma, which could either be a result of astrocyte ApoE knockout affecting peripheral levels or to a small decrease in hepatic production considering that a small number of cells express both ALDH1L1 and APOE in liver[25] (Fig. 2F). APOE4 and APOE3 animals
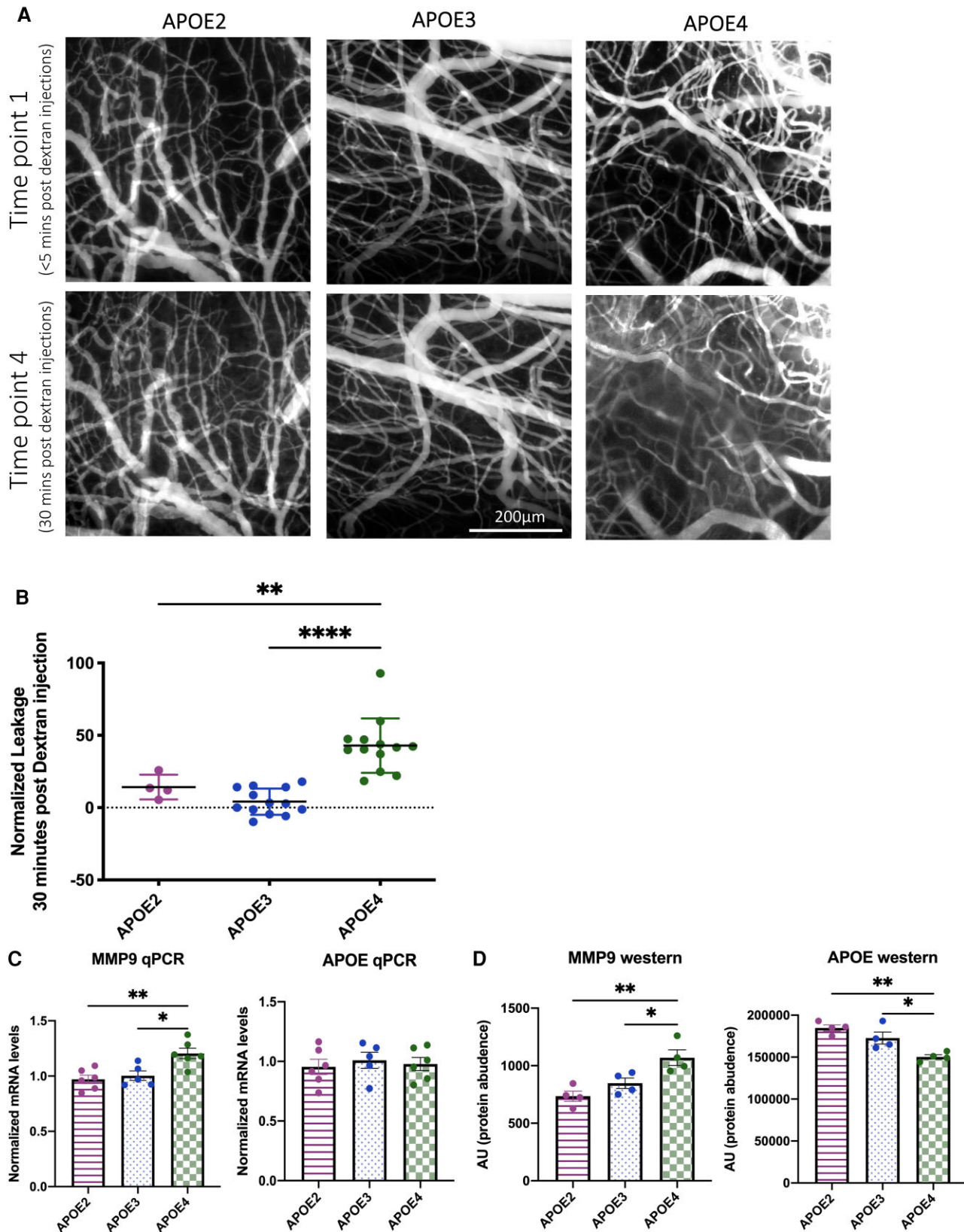
Figure 1 ApoE4-TR mice have an impaired BBB compared with ApoE3-TR and ApoE2-TR mice. (**A**) Multiphoton microscopy of 40 kDa fluorescein conjugated dextran in 9-month-old TR-*APOE2*, TR-*APOE3* and TR-*APOE4* mice. Images are a z-projection of ~120 μm of cortex. (**B**) Quantification of leakage ANOVA [$F(2,27) = 25.03$, $P < 0.0001$]. (**C**) Analysis of whole brain mRNA levels show an increase in MMP9 in APOE4 animals ANOVA [$F(2,14) = 9.086$, $P = 0.0030$] and APOE mRNA levels are unchanged between the three APOE genotypes. (**D**) Analysis of whole brain protein levels of MMP9 show an increase in MMP9 in APOE4 animals compared with APOE2 and APOE3 animals one-way ANOVA [$F(2,9) = 10.01$, $P = 0.0052$] and a decrease in APOE protein levels in the APOE4 animals as compared with the APOE2 and APOE3 animals APOE ANOVA [$F(2,9) = 12.84$, $P = 0.0023$]. *Post hoc* test results are represented as stars *$P < 0.05$, **$P < 0.01$, ***$P < 0.001$, ****$P < 0.0001$.
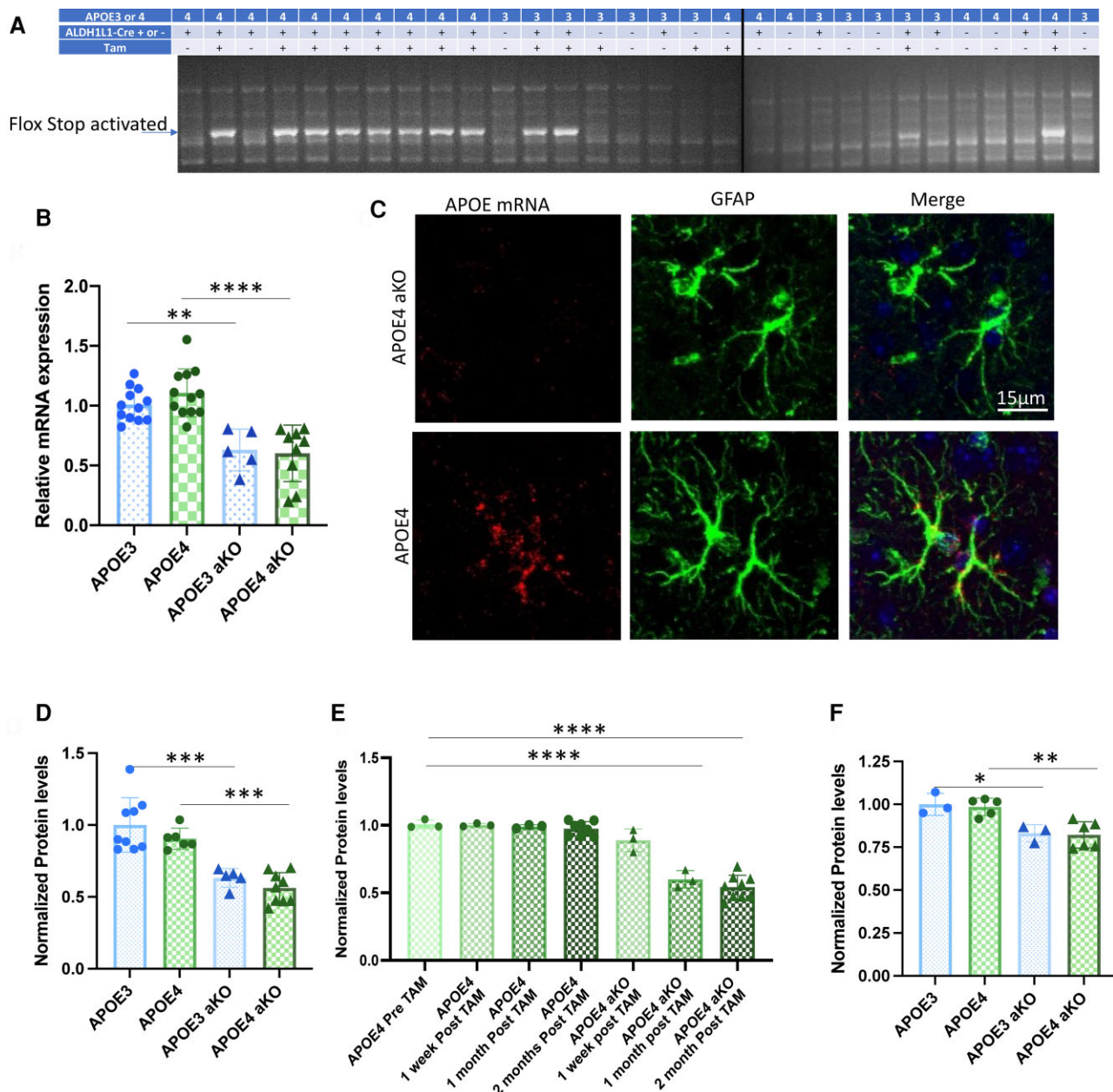
Figure 2 Tamoxifen injection induces a lasting knockout of APOE from astrocytes specifically. (A) PCR of the flox stop site indicates that CRE recombination has occurred in animals that have the ALDH1L1 CRE driver and have been injected with tamoxifen. No recombination event was observed in mice lacking the driver (ALDH1L1-Cre−) or injected with corn oil vehicle only (Tam−). (B) APOE qPCR shows a 40–50% decrease in APOE mRNA in the brain parenchyma after knocking down APOE expressing in astrocytes compared with mice expressing APOE in all cells ANOVA [$F(3,34) = 16.90$, $P < 0.0001$]. (C) RNAscope shows knockout of APOE mRNA in GFAP astrocytes in the CNS. (D) Western blot shows a 40–50% knock down of APOE protein in astrocyte knockout mice ANOVA [$F(3,35) = 121.05$, $P < 0.0001$]. (E) Western blot shows that APOE4 mice show no effect of tamoxifen injection on APOE levels and that APOE aKO mice show no effect 1 week following tamoxifen injection but that by 1 month APOE protein levels are reduced by 40–50% and this is sustained at 2 months ANOVA [$F(6,25) = 49.36$, $P < 0.0001$]. (F) Western blot shows a 15% knock down of plasma APOE protein in APOE3 aKO and APOE4aKO mice ANOVA [$F(3,13) = 9.571$, $P = 0.0013$].

that have had ApoE knocked out of astrocytes are referred to as APOE4 aKO and APOE3 aKO, respectively.

APOE4/ALDH1L1-Cre Mice and APOE3/ALDH1L1-Cre Mice were imaged by two-photon microscopy 1 month prior and 1 week, 1 month and ~2 months post-injection with tamoxifen to understand how the knock-out of astrocytic ApoE (APOE3 or 4 aKO) affected the integrity of the BBB (Fig. 3A). We found that in APOE4 aKO animals the BBB was permeable to 40 kDa dextran prior to and 1 week following tamoxifen injection but by 1 month after

tamoxifen injection this permeability decreased and the leakage of dextran from blood vessels was similar to APOE3 mice (Fig. 3B, C and E). Mice that did not have ApoE4 knocked out from their astrocytes were still permeable to dextran at 12 months of age (Fig. 3D). APOE3/ALDH1L1-Cre mice were treated likewise and there was no effect of ApoE3 knockout from astrocytes on BBB permeability (Fig. 3D). The latter result suggests that the compromised BBB integrity observed in *Apoe* KO animals is not directly dependent upon the absence of ApoE production by astrocytes in this mouse line,
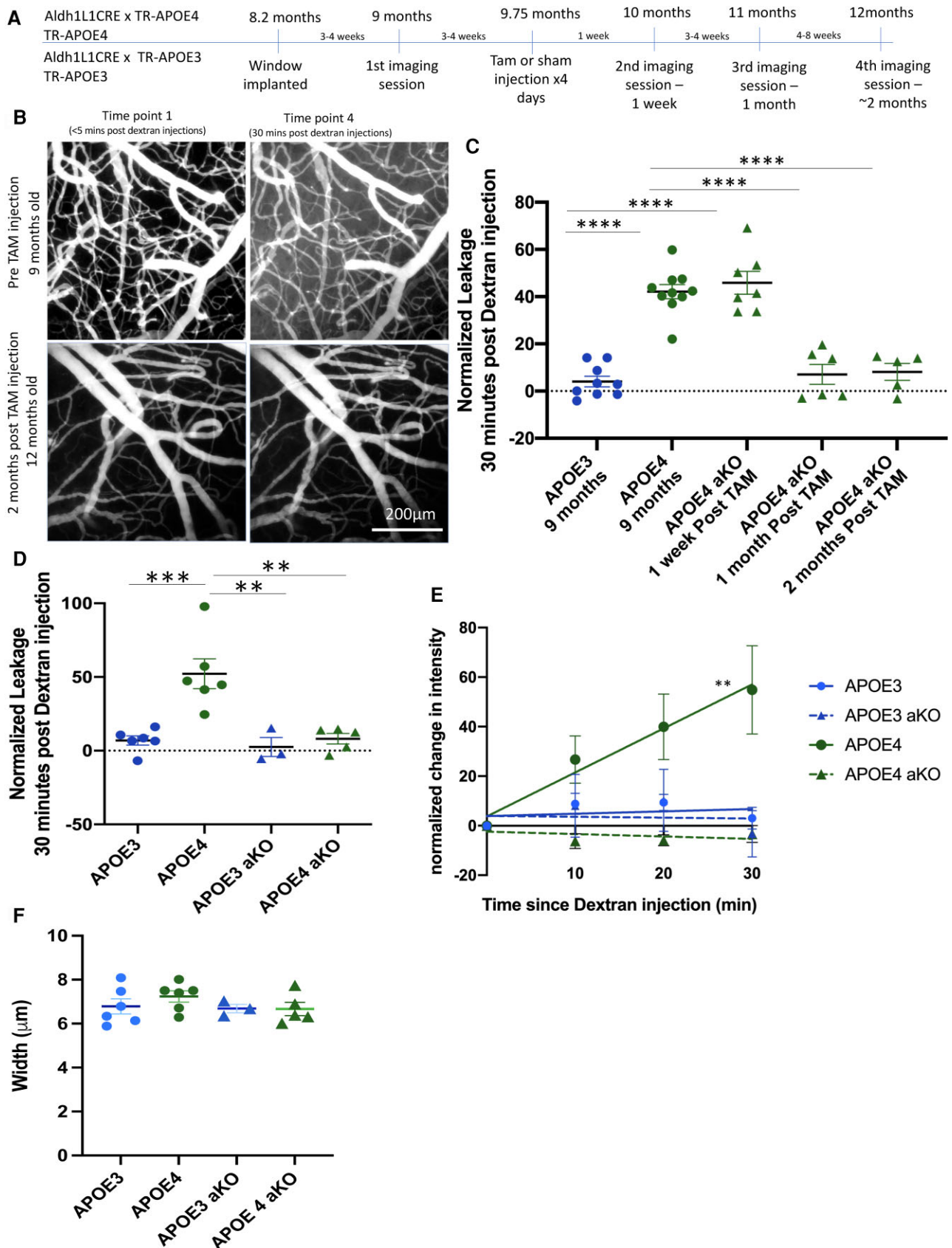
Figure 3 Astrocyte-specific knockout of APOE4 rescues BBB impairments. (**A**) Timeline of *in vivo* studies. (**B**) Multiphoton microscopy or 40 kDa fluorescein conjugated dextran in ALDH1L1CRE×TR-*APOE4* mice before administration of tamoxifen and 2 months post-tamoxifen injection. Images are a z-projection of 100 μm of cortex. (**C**) Quantification of BBB leakage over time in ALDH1L1CRE×TR-*APOE4* compared

(Continued)

highlighting the potential complexity of ApoE associated mechanisms impacting the BBB.

Astrocytic production of ApoE4 leads to aberrant MMP9 expression and tight junction dysfunction

Increases in BBB permeability of small molecules may be indicative of defective structural elements such as tight junctions.[26,27] We therefore assessed tight junction integrity by transmission electron microscopy on cortical sections of APOE3, APOE4, APOE3 aKO and APOE4 aKO mice that were 2 months post-tamoxifen injection (Fig. 4A). Small pullings part of the membranes in tight junctions have been shown to be indicative of tight junction dysfunction[28] (Fig. 4A). We therefore measured the distance between the membranes of tight junctions as well as the width of the endothelium surrounding the lumen in 4–10 blood vessels per mouse. Vessels were chosen if they were ~5–8 μm in diameter and viewed as a cross-section perpendicular to the surface. The first 10 vessels per animal that were found in the cortex were imaged and analysed although not all had visible tight junctions. Where the membranes were so close together that measurement was impossible the distance between tight junction membranes was recorded as 0. We saw a significant increase in the distance between tight junction membranes in the APOE4 mice as compared with APOE3 animals (Fig. 4B). This appears to be mainly driven by an aberrant opening of some tight junctions while others remain intact (Fig. 4C). The APOE4 aKO mice do not show this aberrant opening between tight junction membranes, with similar results as APOE3 mice. We saw no differences in the thickness of the endothelium between the mouse lines (Fig. 4D).

It has been suggested in other models that MMP9 and CYPA mediate ApoE4-driven BBB dysfunction, and that increased MMP9 levels are associated with tight junction breakdown.[10,13,27] Interestingly APOE4 aKO animals have a decreased amount of *Mmp9* mRNA and protein down to the level of APOE3 animals. Furthermore, increased levels of *Mmp9* transcript show a positive correlation with increased levels of *APOE* transcript in APOE4 animals but not APOE3 animals (Fig. 4F). At the protein level the increased level of MMP9 protein in APOE4 animals is also reduced in the APOE4 aKO animals (Fig. 4G) and again the amount of MMP9 protein shows a positive correlation with ApoE4 expression (Fig. 4H). Although there is no significant increase in MMP9 protein in the APOE3 aKO animals there does seem to be a negative correlation between MMP9 protein amount and ApoE3 protein amount (Fig. 4G and H) further indicating a complex relationship between ApoE protein isoform and MMP9.

To begin to investigate the cellular source of these differences in MMP9 and ApoE levels we isolated blood vessels from three mice per group and performed qPCR on these samples as well as RNA extracted from whole forebrain.[21,22] We saw a dramatic enrichment in the levels of *Pecam* in blood vessel preps indicating enrichment of the endothelial cells that are found predominantly in blood vessels in the CNS (Supplementary Fig. 4A). We also saw a ~3-fold enrichment in *APOE* and a ~10-fold enrichment in *Mmp9* in the blood

vessel preps indicating that the vast majority of the *Mmp9* in the CNS is produced in the blood vessel unit and that the blood vessel unit is enriched for cells that produce ApoE (Supplementary Fig. 4B and C). For enrichment analysis qPCR was normalized to the average of the whole brain APOE3 levels.

To understand the effects of ApoE aKO on transcription within the blood vessel we normalized the qPCR for the blood vessel preps to the level of APOE3 blood vessels. We found that there is a 30–40% reduction in the amount of *APOE* mRNA in the aKO animals. As the blood vessel extraction has been shown to contain astrocytes this is not surprising.[22] We also saw a trend ($P = 0.0588$) towards an increase in the amount of *APOE* mRNA in the APOE4 animals as compared with the APOE3 animals, which we do not see in mRNA extracted from whole brain (Supplementary Fig. 4D). We also saw a 100% increase in the amount of *Mmp9* produced in the blood vessels of the APOE4 animals as compared with the APOE3 animals and that this is reduced to the level of APOE3 animals in the APOE4 aKO animals (Supplementary Fig. 4E). We performed as simple linear regression to be sure that this increase is not the result of better blood vessel isolation and found no correlation between *Pecam* and *Mmp9* (Supplementary Fig. 4F).

Astrocyte-produced ApoE4 causes a reduction in astrocyte end-foot protection of blood vessels

Astrocyte end-feet are considered crucial to the formation and maintenance of the BBB in part because of the many secreted factors that have been shown to modulate barrier function through endothelial cells or tight junctions, but also due to the connection they form between the neurons and the blood vessels.[17,26] Using electron microscopy we looked at 10 capillaries per mouse and compared the area of the end foot surrounding the vessel with the outer vessel perimeter measured by drawing a region of interest around the outside of the endothelial cell layer. The examiner was masked to genotype during the image scoring process. We did not exclude vessels where endothelial cell bodies were visible but did exclude vessels that lay parallel to frame rather than perpendicular (as defined as having one diameter more than twice the length of any other diameter). Measurement of the area of the end-foot surrounding the vessel showed that in APOE4 animals there is a reduction of end-foot area and that this is returned to the level of APOE3 animals in APOE4 aKO animals (Fig. 5A). There was no difference between groups in regard to the vessel perimeter (Fig. 5C).

Discussion

Investigating the effect of cell specific production of ApoE on the BBB is important for our understanding the potential functions this apolipoprotein plays in maintaining brain homeostasis. Here we show that humanized APOE4 mice have an increased BBB permeability and that this leakage is rescued as early as 1 month following the knock-out of ApoE4 from astrocytes. Further, we report that APOE4 mice present with disrupted tight junctions, an

Figure 3 Continued

with 9-month TR-APOE3 mice shows a significant leakage prior to and 1 week after tamoxifen injection. At 1 and 2 months after tamoxifen injection, leakage was rescued down to APOE3 levels ANOVA [$F(4,32) = 36.01$, $P < 0.0001$]. (**D**) Quantification of BBB leakage 2 months after tamoxifen injection for TR-*APOE3*, ALDH1L1Cre×TR-*APOE3*, TR-*APOE4* and ALDH1L1Cre×TR-*APOE4* shows that APOE4 mice show significant leakage but that APOE3, APOE3 aKO and APOE4 aKO mice do not ANOVA [$F(3,16) = 36.01$, $P = 0.0003$]. (**E**) Accumulation of fluorescence in the brain parenchyma over time in 12-month APOE3, APOE3 aKO APOE4, and APOE4 aKO mice shows that only APOE4 mice have a slope that is significantly different from 0 [$F(1,26) = 11.57$, $P = 0.0022$]. (**F**) We saw no differences in measured vessel width. Note, not all mice were imaged at all time points due to COVID-19 restrictions and thus *n* numbers fluctuated; however, each mouse is shown as an individual point on the graph (*n* numbers for **E**: APOE3 *n* = 6, APOE4 *n* = 6, APOE3 aKO *n* = 3, APOE4, aKO *n* = 5).
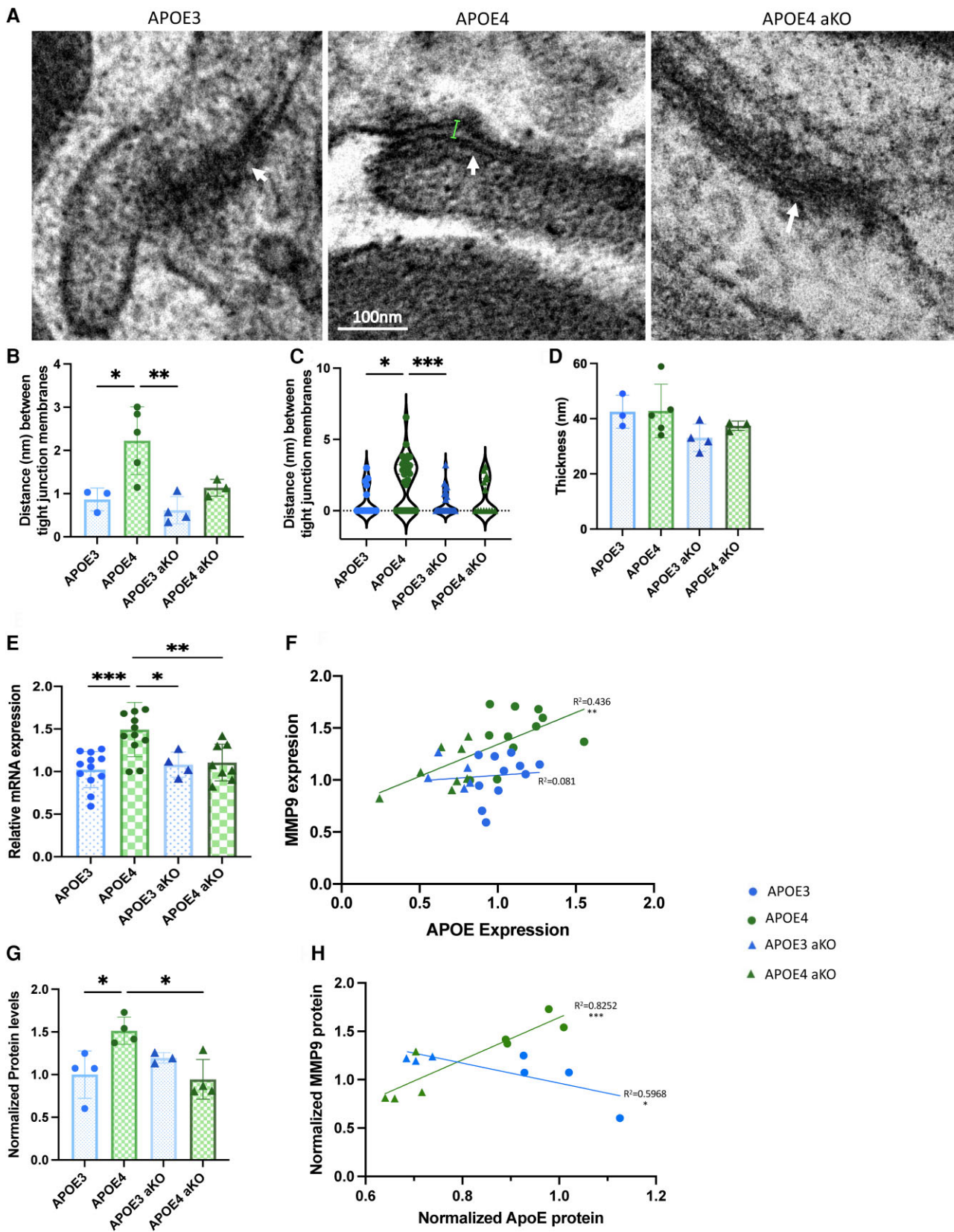
Figure 4 Tight junctions are impaired in ApoE4 mice along with MMP9 expression. (A and **B)** Electron microscopy analysis shows that APOE4 mice show an increased distance (as indicated by a small line) between membranes at tight junctions (white arrows) and that this is ameliorated in APOE4 astrocyte knockout mice both when compared at the mouse level $F(3,11) = 5.926$ $P = 0.0117$ and **(C)** the individual tight junction $F(3,94) = 3.314$ $P = 0.0233$. **(D)** However, we saw no different in the thickness of the endothelium. **(E)** Analysis of whole brain mRNA show that

(Continued)
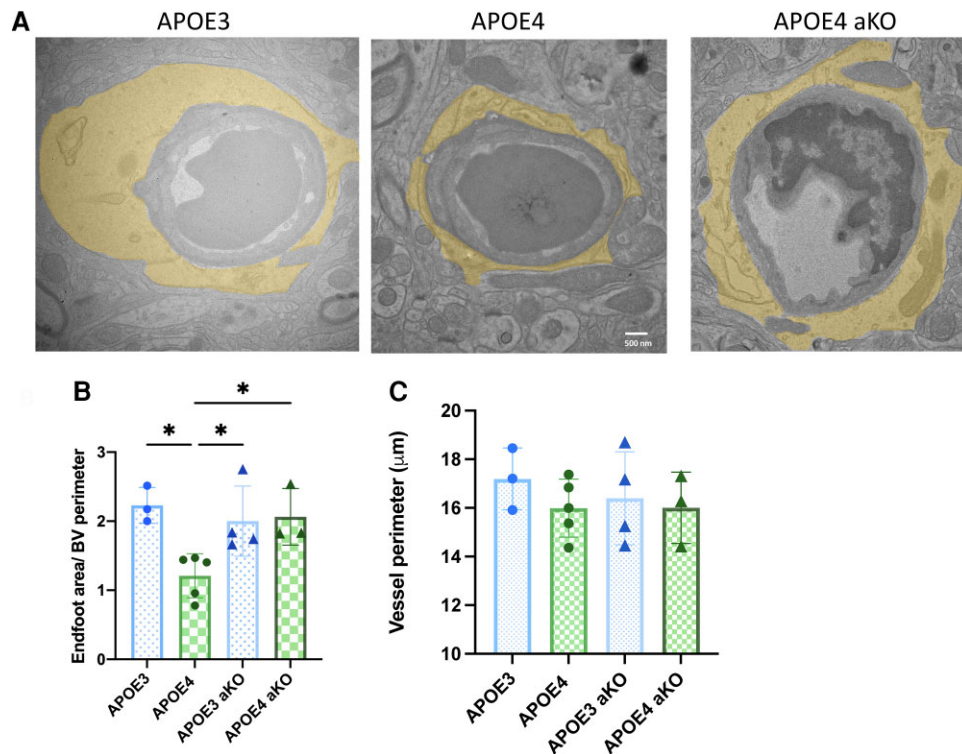
Figure 5 Astrocyte end-feet are impaired in APOE4 mice. (A) Analysis by electron microscopy shows that there is a decreased coverage of astrocytic end-feet (in yellow) in APOE4 mice when compared with APOE3 mice **(B)** and that this is ameliorated in the APOE4 astrocyte knockout mice. $F(3,11) = 5.926$ $P = 0.0117$. **(C)** Vessel perimeter did not differ between groups $F(3,11) = 0.4780$ $P = 0.7040$.

aberrant increase in MMP9 expression and reduced coverage of blood vessels by astrocytic end-feet. These phenotypes were specifically ameliorated by the knock-out of ApoE4 from astrocytes. The present dataset is the first to show the effect of a gain-of-function mechanism by which astrocytically produced ApoE4 appears to negatively impact the BBB and lead to leakage of plasma constituents into the brain. This may be of particular importance in understanding ApoE4-associated vascular dysfunction in the context of Alzheimer's disease, such as the ApoE4 associated risk for amyloid-related imaging abnormalities.[29] Intriguingly, while the current experiments clearly show rescue of the BBB phenotype at both a structural and functional level by reducing astrocyte-produced ApoE4, it has also been shown[30] (and confirmed in these experiments) (Supplementary Fig. 2A and B) that full knockout of *Apoe* from birth leads to a functional and biochemical phenocopy of BBB leakage. Taken together, these results suggest multiple mechanisms by which ApoE protein or the lack of there of influences the integrity of the BBB.

Recent research by Lanfranco *et al.*[31] has shown that ApoE produced by astrocytes and microglia is differently glycosylated and previous research from that group and others has shown that peripherally produced ApoE also undergoes different post translational modifications.[6] These different post-translational modifications lead not only to differences in the size of ApoE lipoprotein particles

but also likely impact the types of receptors ApoE may bind to and thus the downstream effects of those interactions.[32–34]

Of particular interest is the interaction between the different ApoE isoforms and LRP1, which has been shown to be important in the regulation of the cyclophilin A-MMP9 pathway.[35] In agreement with the previous study, we show that APOE4 animals have an increased expression of MMP9. Interestingly previous studies have shown that a lack of ApoE binding to LRP1 leads to activation of the cycolphillin A- MMP9 pathway and that pericyte-derived LRP1 is an important element in this pathway.[13,35] It is thus interesting that knocking-out ApoE4 specifically in astrocytes was sufficient to restore MMP9 mRNA and protein to similar levels seen in APOE3 mice. One possibility is that astrocyte-produced ApoE4 may interact with LRP1 through a different mechanism to mediate BBB changes compared to ApoE3. Cooper *et al.*[36] recently demonstrated that ApoE4 binds LRP1 with the greatest affinity. ApoE lipidation status in the microenvironment of the vessel may also play a role. It has been shown that ApoE interacts with LRP1 differently depending on the source and the lipidation status of the ApoE molecule.[36,37]

It is also possible that this effect of astrocyte derived ApoE4 on BBB dysfunction is independent of LRP1 and leads to MMP9 activation by a different pathway. Interestingly while we see a positive correlation between ApoE4 and MMP9 at the protein level we see a negative correlation between ApoE3 and MMP9 protein (Fig. 4H).

Figure 4 Continued
APOE4 animals have significantly higher expression of MMP9 compared with APOE3 animals but that knock of APOE4 from astrocytes reduces MMP9 expression to the level of APOE3 animals, APOE3 knockout has no effect $F(3,32) = 8.153$ $P = 0.0004$. **(F)** There is a correlation between APOE4 expression and MMP9 expression ($P = 0.0021$) but no correlation between these genes in APOE3 mice. **(G)** Analysis of protein whole brain by western blot shows that there is an increase in MMP9 protein in APOE4 animals compared with APOE3 animals and that astrocyte knock out reduces the MMP9 protein levels of APOE3 animals $F(3,11) = 6.115$ $P = 0.0106$. **(H)** There is a positive correlation at the protein level between APOE4 expression and MMP9 expression ($P = 0.0018$) and a negative correlation between these genes in APOE3 mice ($P = 0.0418$).

This is similar to the effect that we see in the *Apoe* KO animals where the mRNA level is not different from APOE3 animals (Supplementary Fig. 2C and D) but there is an increased level of MMP9 protein compared to APOE3 animals. This highlights the possibility of multiple mechanisms of action of ApoE on MMP9 steady state levels and presumed downstream BBB dysfunction. It is of course possible that were we to have left these animals for longer, BBB dysfunction would have begun to be driven by a different mechanism similar to that seen in the *Apoe* KO animal.

Based on these data and work from other groups, we propose that ApoE4 leads to an increase in MMP9 that results in degradation of tight junction proteins.[10,13,27] We postulate that the increased MMP9 activity leads to an overall destabilization of those structures. Without astrocytic ApoE4, MMP9 levels return to normal and tight junction integrity is restored, preventing BBB leakage. Interestingly, *Apoe* KO animals also show an increase in MMP9 protein and BBB leakage. This indicates that the complete loss of ApoE has negative consequences and suggests non-astrocyte sources of ApoE are critical for BBB maintenance. Altogether, this supports therapeutic strategies that target astrocytes or that convert ApoE4 to ApoeE3 or ApoeE2 may be more effective than reducing overall ApoE levels. It is of course possible that the effect of astrocytic ApoE4 on BBB leakiness is not due totally to an effect on tight junctions but could also arise through a change in transcytosis which has been recently found to be an important mechanism of moment across the BBB.[38,39]

Multiphoton imaging allows us to study the BBB in real time over the course of an animal's lifetime; however, it does have limitations that need to be taken into consideration when assessing this study. Most predominantly is the inflammation that will occur post-surgery, which could lead to an increase in glial activation and changes in brain physiology. For example, the recent paper by Wang *et al.* using the same APOE-KI mice crossed with a tau model saw an ∼80% reduction in CNS APOE mRNA while we see half that at 40%.[18] This could be due to a compensatory or reactive increase in microglial APOE mRNA, a difference in APOE expression due to mouse facility differences,[40] or an increase in APOE mRNA from other cellular sources including those that make up the vascular unit. However, the level of knockdown of ApoE mRNA seen here does agree with previously published datasets showing mRNA levels from each cell type.[7] Another limitation is that this system comprises humanized ApoE in a mouse model where the humanized ApoE interacts with mouse ApoE receptors, modifiers, and lipidators. Mouse ApoE and human ApoE are only 71% identical and these differences could produce effects that are not reflected in humans. However, recent human neuroimaging data[14] similarly reports BBB compromise in *APOE4* carriers indicating insights from this mouse model are relevant to understanding the changes contributing to vascular dysfunction in patients.

In summary, these data are consistent with the hypothesis that ApoE4 has a detrimental gain of function effect on the BBB via astrocytic produced ApoE4. This is strong evidence that the specific source of ApoE is important for its function, suggesting that, at least for astrocytic ApoE, lowering production may be beneficial to maintain BBB integrity in ApoE4 carriers.

Acknowledgements

Funding

Competing interests

E.H. is now employed at Novartis Institute for biomedical research on work unrelated to this manuscript. B.T.H. has a family member who works at Novartis, and owns stock in Novartis; he serves on the SAB of Dewpoint and owns stock. He serves on a scientific advisory board or is a consultant for Avrobio, AZtherapies, Biogen, BMS, Cell Signaling, PPF, Novartis, the US Dept of Justice, Takeda, Voyager, Vigil, W20 group and Seer; his laboratory is supported by Sponsored research agreements with Abbvie, F Prime and research grants from the National Institutes of Health, Cure Alzheimer's Fund, Tau Consortium and the JPB Foundation. The other authors declare no other competing interests.

Supplementary material

Supplementary material is available at *Brain* online.

References

1. Keaney J, Campbell M. The dynamic blood-brain barrier. *FEBS J.* 2015;282(21):4067–4079.
2. Sweeney MD, Sagare AP, Zlokovic BV. Blood-brain barrier breakdown in Alzheimer disease and other neurodegenerative disorders. *Nat Rev Neurol.* 2018;14(3):133–150.
3. Bowman GL, Dayon L, Kirkland R, *et al.* Blood-brain barrier breakdown, neuroinflammation, and cognitive decline in older adults. *Alzheimer's Dement.* 2018;14(12):1640–1650.
4. Cortes-Canteli M, Iadecola C. Alzheimer's disease and vascular aging: JACC focus seminar. *J Am Coll Cardiol.* 2020;75(8):942–951.
5. Linton MF, Gish R, Hubl ST, *et al.* Phenotypes of apolipoprotein B and apolipoprotein E after liver transplantation. *J Clin Invest.* 1991;88(1):270–281.
6. Chernick D, Ortiz-Valle S, Jeong A, Qu W, Li L. Peripheral versus central nervous system APOE in Alzheimer's disease: Interplay across the blood-brain barrier. *Neurosci Lett.* 2019;708:134306.
7. Zhang Y, Chen K, Sloan SA, *et al.* An RNA-sequencing transcriptome and splicing database of glia, neurons, and vascular cells of the cerebral cortex. *J Neurosci.* 2014;34(36):11929–11947.
8. Mahley RW. Central nervous system lipoproteins: ApoE and regulation of cholesterol metabolism. *Arterioscler Thromb Vasc Biol.* 2016;36(7):1305–1315.
9. Banks WA, Reed MJ, Logsdon AF, Rhea EM, Erickson MA. Healthy aging and the blood–brain barrier. *Nat Aging.* 2021;1(3):243–254.
10. Main BS, Villapol S, Sloley SS, *et al.* Apolipoprotein E4 impairs spontaneous blood brain barrier repair following traumatic brain injury. *Mol Neurodegener.* 2018;13(1):17.
11. Nishitsuji K, Hosono T, Nakamura T, Bu G, Michikawa M. Apolipoprotein E regulates the integrity of tight junctions in an isoform-dependent manner in an in vitro blood-brain barrier model. *J Biol Chem.* 2011;286(20):17536–17542.
12. Halliday MR, Rege SV, Ma Q, *et al.* Accelerated pericyte degeneration and blood-brain barrier breakdown in apolipoprotein E4 carriers with Alzheimer's disease. *J Cereb Blood Flow Metab.* 2016;36(1):216–227.

13. Bell RD, Winkler EA, Singh I, *et al*. Apolipoprotein e controls cerebrovascular integrity via cyclophilin A. *Nature*. 2012;485-(7399):512–516.

14. Montagne A, Nation DA, Sagare AP, *et al*. APOE4 leads to blood–brain barrier dysfunction predicting cognitive decline. *Nature*. 2020;581(7806):71–76.

15. Soto I, Graham LC, Richter HJ, *et al*. APOE stabilization by exercise prevents aging neurovascular dysfunction and complement induction. *PLoS Biol*. 2015;13(10):e1002279.

16. Huynh T-PV, Davis AA, Ulrich JD, Holtzman DM. Apolipoprotein E and Alzheimer disease: The influence of apoE on amyloid-β and other amyloidogenic proteins. *J Lipid Res*. 2017;58(5):824–836.

17. Michinaga S, Koyama Y. Dual roles of astrocyte-derived factors in regulation of blood-brain barrier function after brain damage. *Int J Mol Sci*. 2019;20(3):571.

18. Wang C, Xiong M, Gratuze M, *et al*. Selective removal of astrocytic APOE4 strongly protects against tau-mediated neurodegeneration and decreases synaptic phagocytosis by microglia. *Neuron*. 2021;109:1657–1674.e7.

19. Huynh TPV, Wang C, Tran AC, *et al*. Lack of hepatic apoE does not influence early Aβ deposition: Observations from a new APOE knock-in model. *Mol Neurodegener*. 2019;14(1):37.

20. Hudry E, Dashkoff J, Roe AD, *et al*. Gene transfer of human Apoe isoforms results in differential modulation of amyloid deposition and neurotoxicity in mouse brain. *Sci Transl Med*. 2013;5-(212):212ra161.

21. Bennett RE, Hu M, Fernandes A, *et al*. Tau reduction in aged mice does not impact microangiopathy. *Acta Neuropathol Commun*. 2020;8(1):137.

22. Boulay A-C, Saubaméa B, Declèves X, Cohen-Salmon M. Purification of mouse brain vessels. *J Vis Exp*. 2015;105:e53208.

23. Bell RD, Winkler EA, Sagare AP, *et al*. Pericytes control key neurovascular functions and neuronal phenotype in the adult brain and during brain aging. *Neuron*. 2010;68(3):409.

24. Petros AM, Korepanova A, Jakob CG, *et al*. Fragment-based discovery of an apolipoprotein E4 (apoE4) stabilizer. *J Med Chem*. 2019;62(8):4120–4130.

25. Almanzar N, Antony J, Baghel AS, *et al*. A single-cell transcriptomic atlas characterizes ageing tissues in the mouse. *Nature*. 2020;583(7817):590–595.

26. Engelhardt S, Patkar S, Ogunshola OO. Cell-specific blood-brain barrier regulation in health and disease: a focus on hypoxia. *Br J Pharmacol*. 2014;171(5):1210–1230.

27. Hartz AMS, Bauer B, Soldner ELB, *et al*. Amyloid-β contributes to blood-brain barrier leakage in transgenic human amyloid precursor protein mice and in humans with cerebral amyloid angiopathy. *Stroke*. 2012;43(2):514–523.

28. Knowland D, Arac A, Sekiguchi K, *et al*. Stepwise recruitment of transcellular and paracellular pathways underlies blood-brain barrier breakdown in stroke. *Neuron*. 2014;82(3):603–617.

29. Pankiewicz JE, Sadowski MJ. APOE genotype and Alzheimer's immunotherapy. *Oncotarget*. 2017;8(25):39941.

30. Methia N, André P, Hafezi-Moghadam A, Economopoulos M, Thomas KL, Wagner DD. ApoE deficiency compromises the blood brain barrier especially after injury. *Mol Med*. 2001;7(12):810.

31. Lanfranco MF, Sepulveda J, Kopetsky G, Rebeck GW. Expression and secretion of apoE isoforms in astrocytes and microglia during inflammation. *Glia*. 2021;69(6):1478–1493.

32. Lane-Donovan C, Herz J. ApoE receptors, and the synapse in Alzheimer's disease. *Trends Endocrinol Metab*. 2017;28(4):273–284.

33. Zhao N, Liu C-C, Qiao W, Bu G. Review apolipoprotein E, receptors, and modulation of Alzheimer's disease. *Biol Psychiatry*. 2018;83:347–357.

34. Lanfranco MF, Ng CA, Rebeck GW. ApoE lipidation as a therapeutic target in Alzheimer's disease. *Int J Mol Sci*. 2020;21(17):1–19.

35. Nikolakopoulou AM, Wang Y, Ma Q, *et al*. Endothelial LRP1 protects against neurodegeneration by blocking cyclophilin A. *J Exp Med*. 2021;218(4):e20202207.

36. Cooper JM, Lathuiliere A, Migliorini M, *et al*. Regulation of tau internalization, degradation, and seeding by LRP1 reveals multiple pathways for tau catabolism. *J Biol Chem*. 2021;296: 100715.

37. Holtzman DM, Herz J, Bu G. Apolipoprotein E and apolipoprotein E receptors: Normal biology and roles in Alzheimer disease. *Cold Spring Harb Perspect Med*. 2012;2(3):a006312.

38. Andreone BJ, Chow BW, Tata A, *et al*. Blood-brain barrier permeability is regulated by lipid transport-dependent suppression of caveolae-mediated transcytosis. *Neuron*. 2017;94(3):581.

39. Yang AC, Stevens MY, Chen MB, *et al*. Physiological blood–brain transport is impaired with age by a shift in transcytosis. *Nature*. 2020;583(7816):425.

40. Burberry A, Wells MF, Limone F, *et al*. C9orf72 suppresses systemic and neural inflammation induced by gut bacteria. *Nature*. 2020;582(7810):89–94.